

Applications

Performance of a Mesoscale Liquid Fuel-film Combustion-driven TPV Power System

Yueh-Heng Li¹, Yung-Sheng Lien¹, Yei-Chin Chao^{1*,†} and Derek Dunn-Rankin^{2**,†}¹Institute of Aeronautics and Astronautics, National Cheng Kung University, Tainan, 701, Taiwan, ROC.²Department of Mechanical and Aerospace Engineering, University of California, Irvine, California, USA

Combustion-driven thermophotovoltaic (TPV) systems have obtained increasing attention in recent decades, but most studies have focused on developing narrowband photovoltaic cells and selective emitters. In terms of the heat source, conventional combustion configurations and light gaseous fuels are extensively utilized in macro- or meso-scale TPV power systems to simplify thermal management and mechanical fabrication. As far as miniaturization is concerned, however, fuelling these systems with liquid hydrocarbons would provide inherent advantages of high energy density and low volatility. Liquid fuels also promise easy and safe fuel recharging for small-scale power systems. In this paper, a central porous-medium combustor was employed in a small scale TPV power system. The combustor incorporated an emitting chamber wall and a heat recuperator. The radiant efficiency and overall efficiency were compared using different liquid hydrocarbon fuels in the system. The electric output characteristics of the combustion driven TPV system have been investigated to demonstrate the feasibility of a GaSb cell-based TPV power system and to provide design guidance for mesoscale liquid-burning TPV systems. Copyright © 2008 John Wiley & Sons, Ltd.

KEY WORDS: thermophotovoltaic (TPV); GaSb PV cells; porous medium; fuel-film; mesoscale

Received 2 July 2008; Revised 17 October 2008

INTRODUCTION

The development of mesoscale power devices is motivated by the increasing need and demand for smaller scale and more energy dense power sources. Traditional batteries have failed to satisfy high-density-energy demand, often causing serious logistical mission constraints and diminishing overall portable device performance. Minimizing mass and volume have

also become important criteria in the growing trend toward the miniaturization of both mechanical and electromechanical engineering devices.

Before attempting to develop new mesoscale electrical power supplies, it is natural to evaluate the currently available technologies. Batteries are the predominant technology in most applications, but the use of batteries for micro-devices has presented various disadvantages. Batteries have a substantial environmental impact, high cost, and most importantly, relatively low gravimetric (Wh/kg) and volumetric (Wh/L) energy densities. State-of-the-art primary batteries reach up to 1300 Wh/kg and 700 Wh/L and rechargeable up to 400 Wh/L and 300 Wh/kg.¹ These highest performing batteries are expensive, are limited in their peak power

* Correspondence to: Yei-Chin Chao, IAA, National Cheng Kung University, No.1, Ta-Hsueh Rd., Tainan, 701, Taiwan, ROC.

[†]E-mail: ycchao@mail.ncku.edu.tw

** Correspondence to: Derek Dunn-Rankin, University of California at Irvine, Irvine, California 92697, USA.

[†]E-mail: ddunnran@uci.edu

delivery, and are often constrained in size to avoid thermal management issues. Therefore, the use of combustion processes for electric power generation is known to have enormous advantages over conventional electrochemical batteries in terms of power generation per unit volume and energy storage per unit mass, even when the conversion efficiency in the combustion process from thermal energy to electrical energy is taken into account. Interest has grown in the last few years in the miniaturization of combustors as components of energy systems, aiming at the possible replacement of conventional batteries with liquid fuelled ones.²⁻⁴ The primary incentive is the relatively high energy density of liquid fuels with respect to conventional batteries, as shown in Table I. Even accounting for additional system volume and a rather inefficient overall conversion of chemical energy to electricity, a liquid fuel approach would be superior by at least one order of magnitude, not to mention the advantage of the ease of recharging and storage stability. The challenges to develop such a system are numerous, including the identification of promising energy conversion schemes to convert the thermal energy into electricity, effective fuel delivery, efficient heat recuperation, and thermal management.

With regard to mesoscale combustion systems, no universal definitions of mesoscale and microscale exist. We consider the term mesoscale to signify combustor diameters from a few millimeters to about one centimeter. The term microscale indicates that the combustor diameter is smaller than the quench distance of flames for the given fuel (approximately a length scale of one millimeter for stoichiometric hydrocarbon flames at atmospheric pressure). Much of the early and current research on mesoscale power generation has focused on the microscale.^{5,6} However, mesoscale combustion has received increasing attention in recent years because of many potential applications.⁷⁻⁹ For example, a mesoscale power generation system could not only supply electrical power for personal electronics but also power small thrusters or rockets. Mesoscale combustion is also useful for gaining insight into combustion phenomena at moderate scales as a step

toward developing high-power density, microscale systems.

Thermophotovoltaic (TPV) devices convert radiant heat directly into electrical power, and TPV cogeneration systems, where the waste heat is also utilized, has spread into the small scale.^{10,11} Most TPV power systems utilize hydrogen and gas hydrocarbons for fuel, but not liquid hydrocarbons so far. Furthermore, recent investigations have emphasized the application and improvement of selective emitters^{12,13} and narrow-band photovoltaic (PV) cells.¹⁴ However, the overall efficiency of a TPV system is the product of the efficiencies of the PV cells and the radiation source, consisting of the burner and the emitter. Amano *et al.*¹⁵ further pointed out that a special burner for a TPV system should include an emissive emitter and an excellent heat exchanger for high efficiency. Qiu and Hayden¹⁶ asserted that a major energy loss in TPV generation arises from the limited conversion of fuel energy to photon convertible radiation. Therefore, it is essential to develop burner/radiator devices that maximize conversion of fuel to useful radiation energy in order to realize energy efficient TPV systems.

Advances in exquisite micromachining have made feasible and achievable the fabrication of moderate size emitters and PV cells for the miniaturization of TPV power systems. The crucial factor remaining is to successfully design a mesoscale combustor appropriate for TPV systems. The principal obstacles encountered in the combustor miniaturization are inadequate residence time for complete combustion and high rates of heat transfer from the combustor. Along with these obstacles, fuel evaporation leads to another challenge. Liquid fuels must receive sufficient thermal energy for evaporation. Adequate evaporation has been realized in small combustors by multiplexed electrosprays⁴ and fuel-film systems¹⁷, but the application and arrangement of electrosprays in small combustors is restricted by the confined space. Similarly, covering the chamber wall with a fuel-film conflicts with the necessity for a strongly emitting chamber wall. Therefore, to design a new small-scale combustor for liquid fuel burning is

Table I. Comparison of the energy density of natural gases, liquid fuels, and a conventional battery with an assumed 10% efficiency of conversion of fuel chemical energy to electricity

	Methane ($\eta = 0.10$)	Propane ($\eta = 0.10$)	Pentane ($\eta = 0.10$)	Heptane ($\eta = 0.10$)	Lithium-ion battery
Power density (MJ/kg)	5.55	5.04	4.69	4.68	0.45

Assumed conversion efficiency $\eta = 10\%$ for all hydrocarbon fuel.

important in the development of a miniature TPV power system.

EXPERIMENTAL SECTION

Porous medium fuel-film combustor

The priority of designing a mesoscale liquid-fuel-burning driven TPV system is to have a proper combustor, which not only has a flame stabilized inside the chamber but also doubles as an effective emitter of thermal radiation. The fuel-film concept has been demonstrated as a good approach to stably and continuously burn liquid fuels in a confined space.^{18,19,20} However, for applying fuel film combustion in a TPV system, where filming the wall is disadvantageous, a porous medium was incorporated as the primary fuel

surface. A porous medium provides a liquid-film-surface area large enough to produce the necessary fuel vaporization rates and it provides thermal recuperation between the liquid fuel and the flame it supports. The medium also acts as a fuel wick. For these reasons, the porous-fed fuel-film concept is a promising approach for small-scale TPV systems. Figure 1(a) shows a schematic drawing of a miniature liquid film combustion chamber. The main chamber and a liquid-fuel trough are separated by a porous medium. Liquid hydrocarbon fuel is injected smoothly from two inlet ports into the fuel trough using a syringe pump, which provides continuous fuel inlet in range of a few c.c.-per-hour. The air, metered by an electronic flowmeter, is injected tangentially above the fuel ports. Swirling air entering a cylindrical chamber draws the liquid fuel through the porous medium and generates a film on the surface. The swirl also provides a mechanism

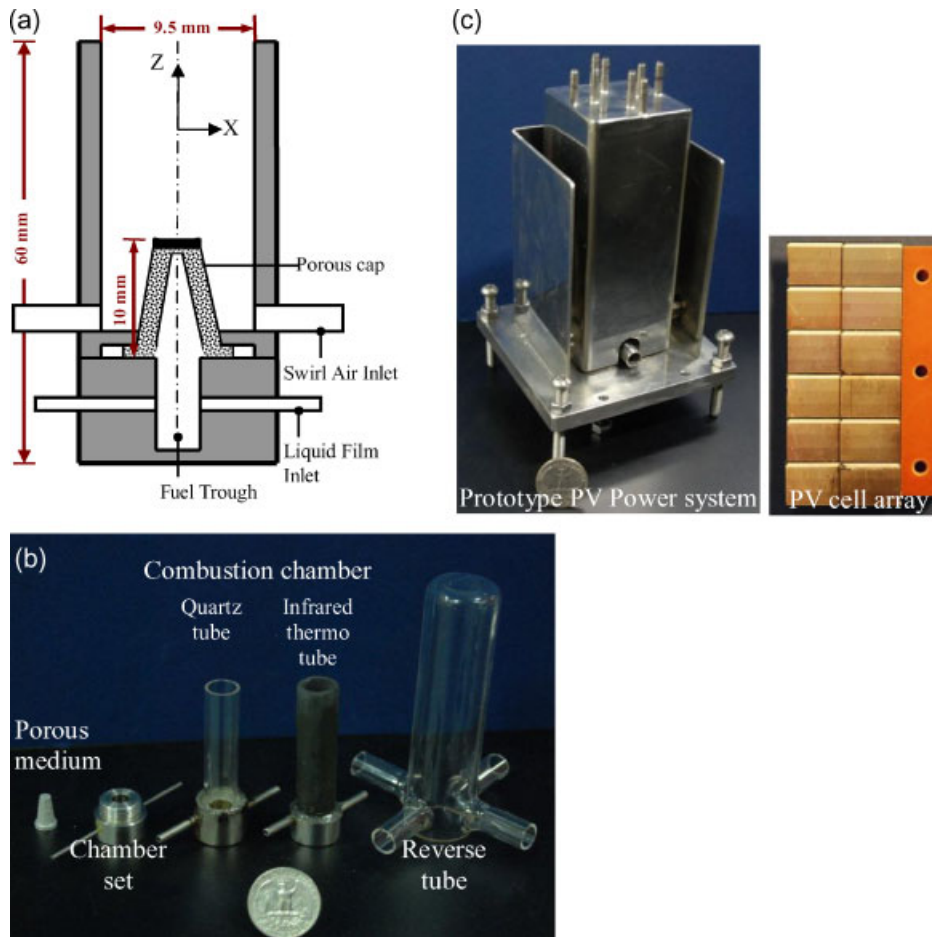


Figure 1. (a) and (b) Schematic diagram and photograph of the experimental combustor, and (c) photograph of the prototype TPV power system

(recirculation) whereby the flame can be stabilized. The swirl system mainly enhances the mixing rate and increases the residence time in the small-scale combustor in order to overcome the deleterious effects caused by the high surface-to-volume ratio. Furthermore, liquid fuel filming on the porous medium produces a large area for vaporization, and the metal porous medium can successively absorb heat from the flame as is needed for fuel evaporation.

The combustion chamber was fabricated using standard machine shop equipment. It consists of only three parts: (1) a combustion chamber of 9.5 mm inside diameter (ID), (2) a chamber set with a fuel trough of 10 mm ID, and (3) a porous medium, shown photographically in Figure 1(b). The combustion chamber was made of an infrared thermal tube 60 mm in length and 3 mm in thickness. The bronze porous medium has a truncated conical shape 4 mm diameter on top, 6.5 mm diameter at the base, and 10 mm long; it has a pore size of approximately 20 μm . The system does not involve any moving parts and it is straightforward to fabricate and assemble. As a result, it can be considered for use in commercial electronics and mesoscale devices, where convenience and low cost, reliable operation, and low maintenance cost are critical.

Emitters and photovoltaic cells

The emitter is another key component in the design of small TPV power devices. The chamber wall acts to confine the flame and as an emitter to convert heat energy from the combustion into radiation. The choices for wall materials are between those that act either as broadband emitters or selective emitters. Although selective emitters exhibit high emittance in the spectral range usable for specific PV cells, broadband emitters (e.g. infrared thermal tubes) have good emissivity and high temperature reliability. Furthermore, compared with other rare earth oxide selective emitters such as Er_2O_3 (erbium) and Yb_2O_3 (ytterbium),^{12,13} it is easier to fabricate broadband emitters into a cylindrical shape. Hence, the infrared thermal tube chosen is made from a mixture of Al_2O_3 and ZrO_2 . It is a typical broadband emitter that operates effectively at temperatures between 900–1400 K. Figure 2 displays the radiation of the infrared thermal tube measured by a monochromator and a photoreceiver. The result shows the highest radiation intensity congregates within the wavelength range between 1300 and 2100 nm.

The emitter has low thermal conductivity, yet the radiation intensity of the emitter is proportional to its

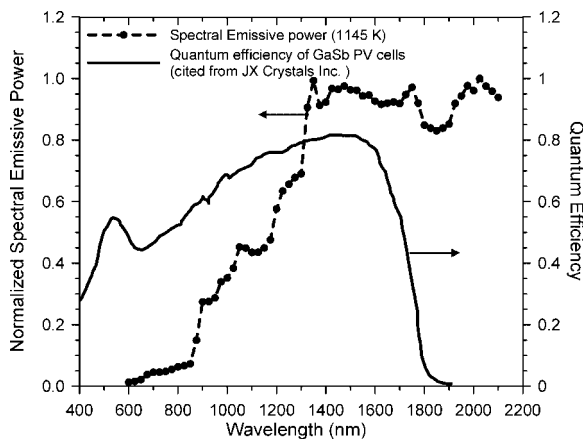


Figure 2. Normalized spectral emissive power of the present thermal tube and quantum efficiency of GaSb PV cells

surface temperature. Accordingly, a fully aerated flame burning close to the emitter surface that heats the surface to incandescence is necessary. Radiant burner design encourages a high surface temperature, while conventional gas burner design often requires minimizing the effect of high burner temperature. It is expected that increasing the combustion air temperature further will considerably increase the useful radiation output.

Choosing a proper photovoltaic cell array is essential in the design of any mesoscale TPV power device. Silicon solar cells have good quantum efficiency in the 300–1200 nm wavelength, while GaSb PV cells have good quantum efficiency in the 700–1800 nm wavelength, as displayed in Figure 2. Based on matching the radiation of the emitter, low band GaSb TPV energy conversion was needed in order to simultaneously maximize both the efficiency and the power density. Backside contact-type GaSb PV cells, fabricated by JX Crystals Inc. USA, were connected electrically in series surrounding the emitter. Because only planar GaSb cells are available, the cylindrical array is composed of four cell arrays forming a tube. Each cell array has an area of 18 cm^2 and contains two strings of six series connected cells in parallel (shown in Figure 1(c)).

Instrumentation

Various control and measuring devices, including thermocouples, IR thermometer, gas analyzer, and voltage/current analyzer were installed in the experimental setup. The thermocouples were used to measure the temperature of the flue gases, and the IR thermometer was able to monitor the surface temperature of the emitter. The radiant efficiency was calculated based on the measured radiant output and fuel input rate. The electrical output

Table II. Maximum error in measurement results

Measurement uncertainty	Maximum error
Fuel flow rate	$\pm 2.0\%$
Air flow rate	$\pm 3.0\%$
Temperature	$\pm 3.0^\circ\text{C}$
Gas emission	
CO	$\pm 5.0\%$
NO _x	$\pm 2.4\%$

characteristics of the cells were determined using an I–V analyzer. The combustion efficiency and exhausted gas management were examined by gas emission measurement. The gas analyzer (MRU, VarioPlus) combines NDIR-technology and electrochemical sensors, so that it can detect O₂, CO, NO_x, CO₂, and UHC (unburned hydrocarbon). Table II shows the uncertainties of the measurement techniques.

RESULTS AND DISCUSSION

Burner combustion performance

Understanding the characteristics of a liquid fuel central porous combustor is crucial for creating a compact combustion driven TPV system. Figure 3 exhibits the

combustion modes for various air/fuel flow rates using liquid *n*-heptane. The emitter chamber wall was replaced by transparent quartz tube in order to observe the flame characteristics inside the chamber. Predictably, flames would blow out or quench when air flow rates were too high and liquid fuel would pool on the bottom of the combustion chamber when air flow rates were too low. Between these extremes, there are three combustion modes over the range of operating conditions, including double layer flames, attached-wall flames, and central flames. The double-layer flame mode has a second flame burning on the rim of the combustion chamber due to unburned gas reacting at the exit, and it appears for low air flow rate. In the central flame mode the flame is confined to the centerline of the combustion chamber due to strong swirling air flow. These two combustion modes are not suitable for use in a radiant combustor because they do not heat the emitter wall effectively. In the attached-wall flame mode, the flame sheet attaches to the combustion chamber, and this combustion characteristic meets the fundamental requirement of a radiant burner.

In the liquid fuel-film combustor, the porous medium and the fuel type strongly influence the combustion phenomena and operating range. The porous medium provides a large surface area and heat recuperation for

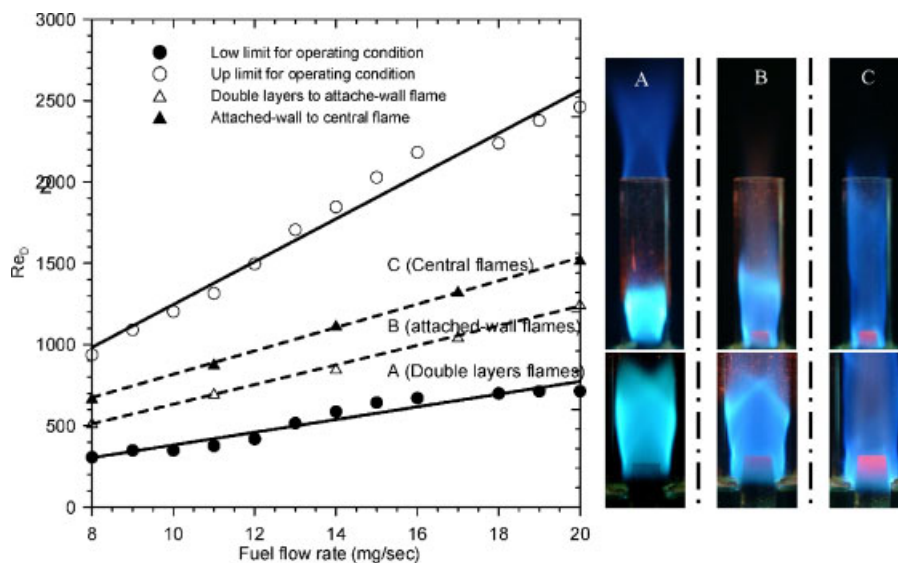


Figure 3. Combustor operation map with three characteristic flame modes: (a) double layers flame, (b) attached-wall flame, and (c) central flame, depending on Re_D , and images showing the corresponding flame structures and closeup views of flame anchoring position onto the stainless steel porous cap

liquid fuel evaporation. Theoretically, effective thermal conductivity of the porous medium filled with fluid is a function of porosity, thermal conductivity of the solid, and thermal conductivity of the fluid. Figure 4 indicates the stable operating envelopes for different fuel types and porosity. As shown in Figure 4(a), the porosity of the porous medium (32, 40, and 48%) does not change the envelope region substantially when using *n*-heptane as the fuel. The regime of stable combustion operation in the small porosity condition is a little larger than that in the large porosity condition. The reason is that the small-porosity porous medium has a greater solid fraction, which produces a larger effective thermal conductivity, so that it can more easily transfer heat from the flame to the fuel. The latent heat of the liquid fuel is the other important influence on porous burner behavior. Figure 4(b) indicates the stable operating envelope using two different fuels, pentane and heptane. The stable operating envelope of pentane is larger than that of *n*-heptane. Owing to its low boiling temperature, pentane can evaporate more easily, so it can run over a wider fuel/air condition. Table III shows the properties of pentane and *n*-heptane, including density, boiling temperature, latent heat, and viscosity. Fuel sorptivity of the porous medium is related to the capillary effect and surface tension. Fuel surface tension and fluid viscosity may influence the spread rate of liquid fuel on the porous surface, but it is not very different between the two fuels. Furthermore, in this case, the feeding pressure from the syringe pump dominates over these passive effects.

Emitter radiant characteristics

Uniform and high illumination of an emitter is essential for good radiant efficiency. Radiant efficiency of the emitter can be defined as

$$\eta_{\text{rad}} = \frac{P_{\text{rad}}}{H_{\text{fuel}}\dot{m}} = \frac{\int_0^{\infty} W_b(\lambda, T)\varepsilon_{\text{GaSb}}S_E d\lambda}{H_{\text{fuel}}\dot{m}}$$

$$= \frac{\sigma T^4 \varepsilon_{\text{GaSb}} S_E}{H_{\text{fuel}}\dot{m}}$$

Table III. Properties of pentane and *n*-heptane

Fuel type	Density (g/cm ³)	Boiling temperature (K)	Latent heat (kJ/kg)	Viscosity (mPa/s)
Pentane	0.626	308	342	0.240
<i>n</i> -Heptane	0.684	372	320	0.386

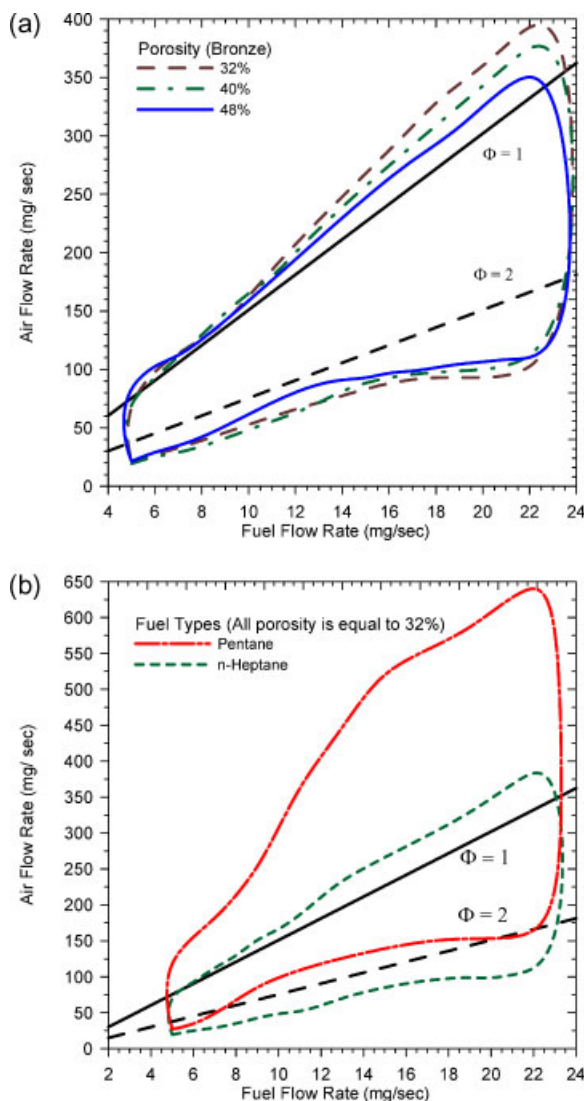


Figure 4. Stable operating envelopes for the combustor with (a) different porosity and (b) different fuel types

where P_{rad} is the net radiation power emitted by the emitter, H_{fuel} the fuel heating value, \dot{m} the fuel mass flow rate, σ is the Stefan–Boltzmann constant ($5.67 \times 10^{-8} \text{ W/m}^2/\text{K}^4$), and S_E is the emission area of the emitter. As can be seen from the definition above, radiant efficiency is strongly related to surface

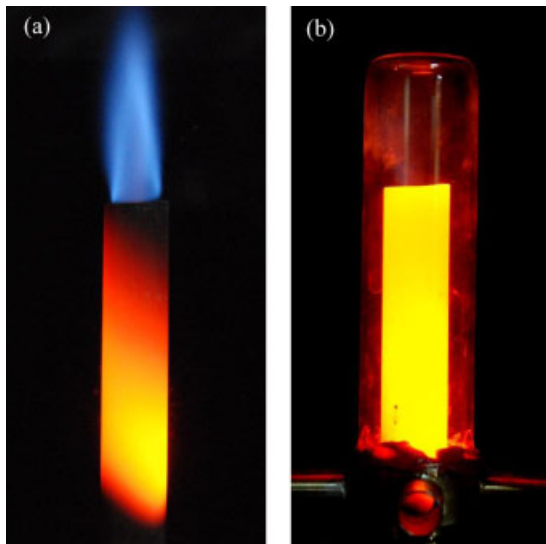


Figure 5. Photographs of combustion chamber operation (a) without a reverse tube, and (b) with a reverse tube

temperature of the emitter according to Planck's rule. The radiant efficiency can be estimated by the measured surface temperature. Miniature combustors have the inherent drawbacks of short residence time and potentially incomplete combustion. Incomplete combustion reduces heat release, but an even more detrimental effect of short residence time is that heat transfer to the emitter is reduced, producing an uneven and faded illumination of the emitter, as shown in Figure 5(a). The bright illumination appears at the bottom of the emitter and exposes the position of flame attachment. The illumination image has a spiral pattern along the emitter caused by strong swirling air flow, and a long flame plume exists near the chamber exit. For ameliorating this situation, a reverse tube was implemented for redirecting the hot product gas and reheating the emitter. Figure 5(b) indicates the intensity and uniformity of illumination on the emitter after this improvement. In addition, flames now completely burn inside the chamber. In order to examine the uniformity of illumination, surface temperature along the emitter was measured by IR thermometer. Figure 6 shows the temperature distribution along the emitter for the same fuel input (11 mg/s) and varied equivalence ratios. The figure shows that the emitter has uniform and high temperature distribution when the equivalence ratio approaches the stoichiometric condition. Burning in the fuel-rich condition may be necessary to provide sufficient fuel evaporation but this sacrifices the opportunity of heating the emitter and leads to reduced emitter temperature. Fortunately,

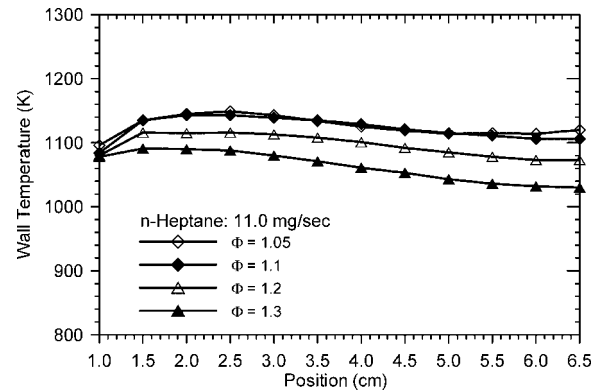


Figure 6. Measured wall temperature distribution along the axial direction in air of 165 mg/s and fuel of 11 mg/s for pentane and *n*-heptane

the evaporation heat requirement can be adjusted because it is related to fuel characteristics. Figure 7 indicates the temperature measurement in a flow condition of air at 165 mg/s and fuel at 11.0 mg/s for pentane and *n*-heptane. Use of different liquid hydrocarbons seems not to produce obvious differences except in the no-reverse-tube case. Pentane can prematurely evaporate due to its low boiling temperature, so that the flame attachment position locates more upstream than occurs when the fuel is *n*-heptane. The temperature distribution along the emitter without a reverse tube has a steep decreasing tendency, while that with a reverse tube has slight temperature variation. It appears that a reverse tube promotes the illumination and uniformity of the emitter. Another option might be to increase the number of tangential air inlets to enhance swirling intensity and further improve the uniformity of illumination.

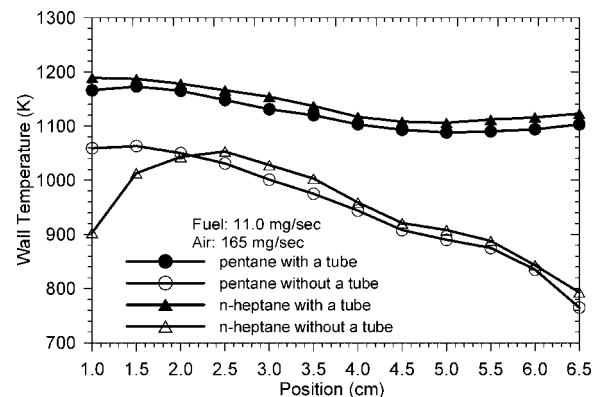


Figure 7. Measured wall temperature distribution along the axial direction in *n*-heptane fuel of 11 mg/s and varied equivalence ratios

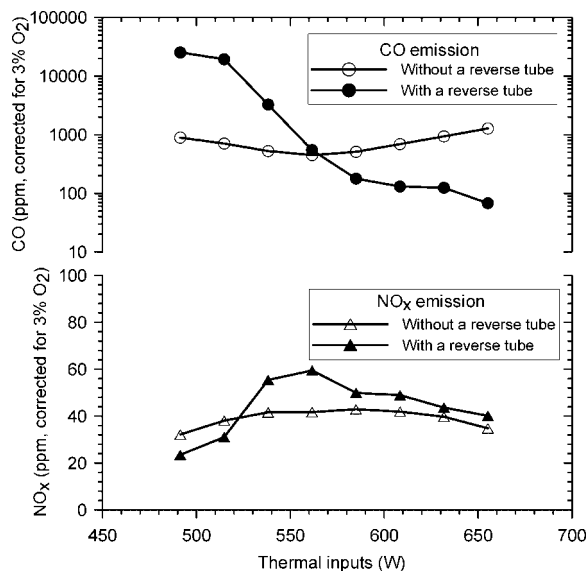


Figure 8. Effect of thermal input on CO and NO_x emissions

Miniaturization with incomplete combustion may be a Pyrrhic victory as the two goals of small combustor and complete combustion are often difficult to reconcile. In order to monitor the chemical efficiency of the present combustion system, measurements were conducted using the gas analyzer to obtain CO₂, CO, O₂, and UHC. Since no other carbon containing species except CO₂, CO, and unburned hydrocarbons were observed in these conditions, the chemical efficiency of methane combustion was defined as the ratio of the measured volume percentage of carbon dioxide and all carbon-containing species. Figure 8 displays the CO and NO_x emissions for different thermal inputs of *n*-heptane and fixed equivalence ratio of 1.1. In the case without a reverse tube, CO and NO_x emissions do not change significantly. The CO emission rises when fuel flow rate increases, but that of NO_x does not. As regards chemical efficiency, all conditions are able to reach 95% conversion. Nevertheless, the reverse tube

produces obvious changes in CO emission. When air and fuel flow rate increase, CO emission sharply decreases, and its corresponding chemical efficiency varies from 82 to 99%. Increase in heat release produces high thermal transfer. Unburned hydrocarbons that pass through the emitter tube can react in the reverse tube since the emitter has high surface temperature and thermal radiation. Relatively speaking, NO_x emission increases only slightly since chemical efficiency also increases. Table IV shows gas emission and the corresponding chemical efficiency for air flow of 165 mg/s and fuel flow of 11 mg/s for pentane and *n*-heptane (thermal input is approximately equal to 515 W). Combustors with a reverse tube for both fuels have low CO emissions and are accompanied by relatively high chemical efficiencies. Chemical efficiency and gas emission do not show large differences between pentane and *n*-heptane. The reverse tube reinforces thermal recuperation and prolongs residence time. It does not only brighten the illumination of an emitter, but also enhances chemical efficiency.

Systematic efficiency demonstration

In order to evaluate the feasibility of using the proposed miniature central porous combustor in a TPV system, GaSb PV cells are employed to collect illumination emission and convert it into electricity. The electrical power output of the prototype mesoscale liquid fuel TPV system incorporating GaSb cell modules is then measured for various equivalence ratios and different fuel types. The prototype TPV system consists of the central-porous medium combustor surrounding by four solar cell modules. Figure 9 shows the maximum electrical power output for different equivalence ratio and fuels. For the identical fuel condition, maximum electrical power output increases depending upon increase in thermal input. It appears that as fuel/air ratio moves toward the stoichiometric condition, power output correspond-

Table IV. Gas emissions measured by GA analyzer and chemical efficiency in different conditions

Condition	Pentane without a cap	Pentane with a cap	<i>n</i> -Heptane without a cap	<i>n</i> -Heptane with a cap
CO ₂ (%)	4.07	4.25	3.61	4.55
CO (ppm) ^a	557.1	120.8	665.7	86.4
NO _x (ppm) ^a	34.9	36.6	34.3	37.3
η _{chem} (%) ^b	97.63	97.92	97.77	98.23

^aEmission refers to 3% oxygen.

^bMeans chemical efficiency.

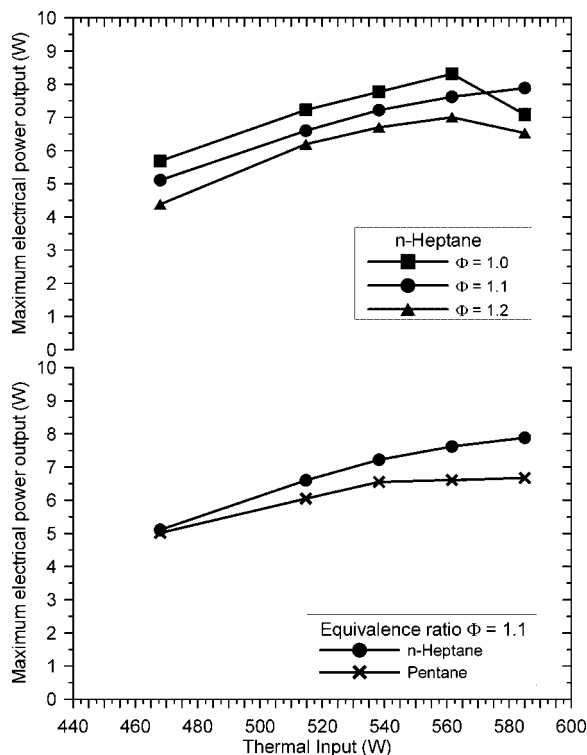


Figure 9. The maximum electrical power output under (a) different equivalence ratios of *n*-heptane, (b) different fuel types

ingly increases due to complete combustion, shown in Figure 9(a). High thermal inputs, however, may increase heat release and thermal transfer in the system. For example, power output at equivalence ratio of 1.1 was curtailed when thermal input rose to a high value. Since high thermal input requires high air flow rate, high flow rate compels the flame attachment point to move downstream. This leads to the emitter lamination fading away, and ends up decreasing electrical power output. Figure 9(b) exhibits the electrical power output for two fuels varying the thermal input, but fixing the equivalence ratio. The TPV system burning *n*-heptane obtains higher power output than that burning pentane. The two fuels have similar energy density and so the difference in electrical power output is due to the particular combustion mode. With a reverse tube, combustion modes inside the chamber couple with fuel parameters, such as latent heat and fuel density. Further observation on flow dynamics inside the tube will help determine the relationship between fuel type and power output.

Estimated from Figure 9, the average overall thermal-to-electricity conversion efficiency for all

conditions is approximately 1%. As the *n*-heptane flow rate is 12 mg/s (thermal input is 561.6 W) and equivalence ratio is 1.0, an electrical power output of 8.3 W has been achieved for the small fuel-film TPV system, corresponding to an overall efficiency of 1.47%, which is twice that obtained by Yang.²¹ Based on maximum electrical power output, the power density of the present prototype TPV power system is a little higher than that of a high-quality, commercially optimized lithium-ion battery. The open-circuit voltage and short-circuit current are 1.81 V and 6.6 A. The fill factor, defined as the ratio of the actual maximum obtainable power to the theoretical power, reaches 0.695. The high efficiency region of the GaSb PV cell spans between 600 and 1700 nm wavelength, but the output of the present emitter ranges between 1300 and 2100 nm, as shown in Figure 2. The non-matching photons are not converted to electricity by the PV cells, but increase their temperature, which further reduces the conversion efficiency. In order to further improve the efficiency of the small fuel-film TPV system, it is necessary to employ lower band gap GaInAsSb PV cells where high quantum efficiency is achieved between 800 and 2400 nm. Furthermore, by means of utilizing a selective emitter in further designs instead of infrared thermal broadband emitters, most of the photons emitted can be located in the short wavelength range with energies greater than the bandgap of the PV cells.

CONCLUSION

A mesoscale liquid-fuel-film combustor with a central porous inlet was proposed for application in a TPV power system. Providing a metal-porous medium can result in increasing contact surface and conduction heat transfer for liquid fuel evaporation as well as inhibition of flame quench. Depending upon the Reynolds number, there are three combustion modes through the conditions, double layer flame, attached-wall flame, and central flame. Only the attached-wall flame is a proper option for application in the TPV power system. In order to produce a uniform illumination of the emitter, a reverse tube is demonstrated. The results show that the chamber wall has uniform illumination and that the flame can be confined inside the chamber. The power output of the PV cell is dependent on combustion efficiency and emitter temperature. Two different liquid fuels are tested. In the prototype design, when the flow rate of

n-heptane is 12 mg/s and equivalence ratio is 1.0, the small fuel-film TPV system is able to deliver a promising electrical power output of 8.3 W, corresponding to an open-circuit electrical voltage of 1.81 V and a short-circuit current of 6.6 A.

REFERENCES

- Linden D. *Handbook of Batteries*. McGraw-Hill: New York, 2002.
- Fernandez-Pello AC. *Proceedings of the Combustion Institute* 2003; **29**: 883–889.
- Dunn-Rankin D, Leal EM, Walther DC. *Progress in Energy Combustion Science* 2005; **31**: 422–465.
- Kyritsis DC, Roychoudhury S, McEnally CS, Pfefferle LD, Gomez A. *Experimental Thermal and Fluid Science* 2004; **28**: 763–770.
- Yuasa S, Oshimi K, Nose H, Tennichi Y. *Proceedings of the Combustion Institute* 2005; **30**: 2455–2462.
- Norton DG, Vlachos DG. *Proceedings of the Combustion Institute* 2005; **30**: 2473–2480.
- Wu M-H, Wang Y, Yang V, Yetter RA. *Proceedings of the Combustion Institute* 2007; **31**: 3235–3242.
- Kyritsis DC, Roychoudhury S, McEnally CS, Pfefferle LD, Gomez A. *Experimental Thermal and Fluid Science* 2004; **28**: 763–770.
- Qiu K, Hayden ACS. *Energy Conversion and Management* 2006; **47**: 365–376.
- Chia LC, Feng B. *Journal of Power Sources* 2007; **165**: 455–480.
- Durisch W, Bitnar B, Mayor, Fritz von Roth J-C, Sigg H, Tschudi HR, Palfinger G. *Applied Energy* 2003; **74**: 149–157.
- Bitnar B, Durisch W, Mayor J-C, Sigg H, Tschudi HR. *Solar Energy Materials and Solar Cells* 2002; **73**: 221–234.
- Nakagawa N, Ohtsubo H, Waku Y, Yugami H. *Journal of the European Ceramic Society* 2005; **25**: 1285–1291.
- Qiu K, Hayden ACS. *Solar Energy* 2003; **74**: 489–495.
- Amano T, Yamaguchi M. *Solar Energy Materials and Solar Cells* 2001; **66**: 579–583.
- Qiu K, Hayden ACS. *Solar Energy Materials and Solar Cells* 2007; **91**: 588–596.
- Sirignano WA, Pham TK, Dunn-Rankin D. *Proceedings of the Combustion Institute* 2002; **29**: 925–931.
- Pham TK, Dunn-Rankin D, Sirignano WA. *Proceedings of the Combustion Institute* 2007; **31**: 3269–3275.
- Li Y-H, Chao Y-C, Amadé NS, Dunn-Rankin D. *Experimental Thermal and Fluid Science* 2008; **32**: 1118–1131.
- Li Y-H. *Development of a meso-scale fuel-film combustor with central-porous fuel inlet*, Ph.D. dissertation. National Cheng Kung University: Tainan, Taiwan, 2008.
- Yang WM, Chou SK, Shu C, Xue H, Li ZW. *Journal of Physics D: Applied Physics* 2004; **37**: 1017–1020.